

Abstract. We analyze three types of rogue wave (RW) clusters for the quintic nonlinear Schrödinger equation (QNLSE) on a flat background. The exact QNLSE solutions are generated using the Darboux transformation (DT) scheme and they are composed of the higher-order Akhmediev breathers (ABs) and Kuznetsov-Ma solitons (KMSs). We analyze the dependence of their shapes and intensity profiles on the eigenvalues and evolution shifts in the DT scheme and on three real quintic parameters. The first type of RW clusters, characterized by the periodic array of peaks along the evolution or transverse axis, is obtained when the condition of commensurate frequencies of DT components is applied. The elliptical RW clusters are computed from the previous solution class when the first m evolution shifts in the DT scheme of order n are equal and nonzero. For both AB and KMS solutions a periodic structure is obtained with the central RW and m ellipses, containing the first-order maxima that encircle the central peak. We show that RW clusters built on KMSs are significantly more vulnerable to the application of high values of QNLSE parameters, in contrast to the AB case. We next present non-periodic long-tail KMS clusters. They are characterized by the rogue wave at the origin and n tails above and below the central point containing the first-order KMSs. We also show that the breather-to-soliton conversion can transform the shape of RW clusters by careful adjustment of the real parts of DT eigenvalues, while remaining parameters are left unchanged.

Quintic equation:
$$i\frac{\partial\psi}{\partial x} + \frac{1}{2}\frac{\partial^2\psi}{\partial t^2} + |\psi|^2\psi - i\alpha H + \gamma P - i\delta Q = 0$$

x – evolution variable, t – transverse variable, $\psi = \psi(x, t)$ is a complex function

$$H[\psi(x, t)] = \psi_{ttt} + 6|\psi|^2\psi_t \quad Q[\psi(x, t)] = \psi_{tttt} + 10|\psi|^2\psi_{ttt} + 30|\psi|^4\psi_t + 10\psi\psi_t\psi_{tt}^*$$

$$P[\psi(x, t)] = \psi_{tttt} + 8|\psi|^2\psi_{tt} + 6|\psi|^4\psi + 4|\psi_t|^2\psi + 10\psi\psi_t^*\psi_{tt} + 20\psi^*\psi_t\psi_{tt} + 10\psi_t^2\psi_t^* + 6\psi_t^2\psi^* + 2\psi^2\psi_{tt}^*$$

I. Periodic arrays of RWs composed by Kuznetsov–Ma solitons

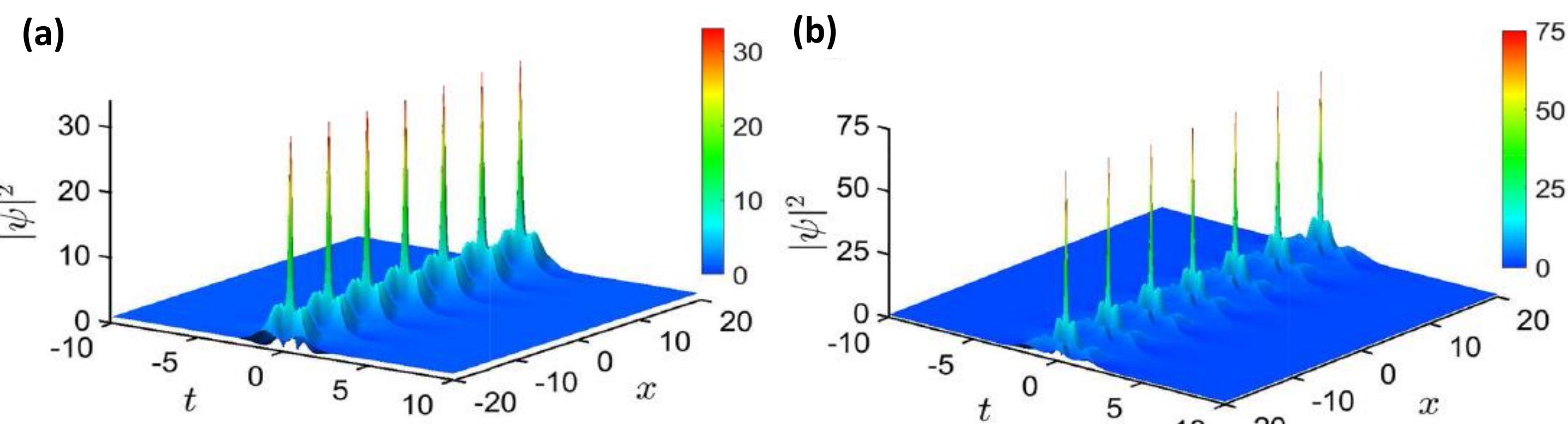


Figure 1: 3D color plots of higher-order Kuznetsov–Ma solitons with commensurate frequency components on a uniform background for pure NLSE ($\alpha = 0, \gamma = 0, \delta = 0$): (a) The second-order DT solution with $v = v_1 = 1.1$, (b) The third-order DT solution with $v = v_1 = 1.1$.

KM solitons are periodic along x-axis: $T_x = \frac{\pi}{v\sqrt{v^2 - 1}}$

Main frequency (first DT component): $\omega_x = \frac{2\pi}{T_x} = 2v\sqrt{v^2 - 1}$

Commensurate frequencies: $\omega_{xj} = j\omega_x$ **Arbitrary v_1 :** $v \equiv v_1$

Imaginary parts of DT eigenvalues for $j \geq 2$: $v_j = \sqrt{\frac{1 + \sqrt{1 + 4j^2v^2(v^2 - 1)}}{2}}$

n^{th} -order DT solution: $\lambda_j = r_j + iv_j, x_j, t_j \quad (1 \leq j \leq n)$

II. Multi-elliptic rogue wave clusters of Akhmediev breathers and Kuznetsov–Ma solitons (KMS and AB MERWC)

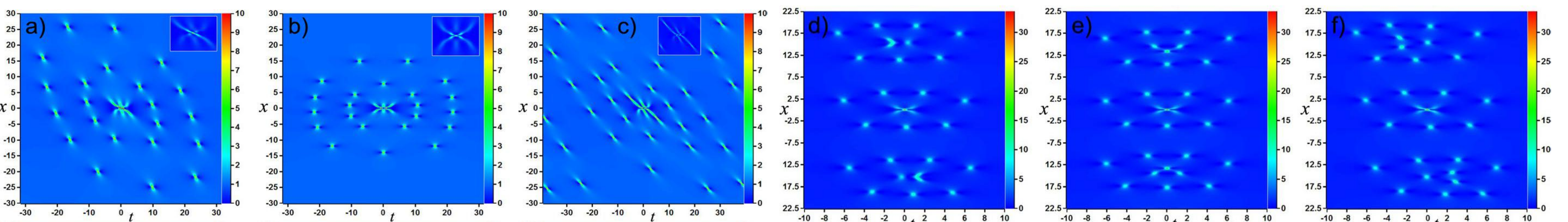


Figure 2: Intensity distributions of the multi-elliptic rogue wave clusters built on the higher-order ABs and KMSs. AB MERWC is calculated for $n = 7, m = 2, \omega = 0.1, x_1 = x_2 = 1$, and: (a) $\alpha = 0.07, \gamma = 0, \delta = 0$, (b) $\alpha = 0, \gamma = 0.07, \delta = 0$, (c) $\alpha = 0, \gamma = 0, \delta = 0.035$. The insets show the actual appearance of the central RW. KM MERWC is computed for $n = 4, m = 1, v_1 = 1.02, x_1 = 1$, and: (d) $\alpha = 0.006, \gamma = 0, \delta = 0$, (e) $\alpha = 0, \gamma = 0.006, \delta = 0$, (f) $\alpha = 0, \gamma = 0, \delta = 0.002$.

Eigenvalues for KMS: $v_j = \sqrt{\frac{1 + \sqrt{1 + 4j^2v^2(v^2 - 1)}}{2}}$

Eigenvalues for AB: $v_j = \sqrt{1 - \frac{j^2\omega^2}{4}}$

Evolution shifts: $x_j = \sum_{l=1}^{\infty} X_{jl}\omega^{2(l-1)} = X_{j1} + X_{j2}\omega^2 + X_{j3}\omega^4 + X_{j4}\omega^6 + \dots$

- KMS/AB of order $n-2m$ at ellipses' center
- m ellipses around the peak
- $2n-1$ KMS1/AB1 on outer ellipse and 4 KMS1/AB1 less on each following ring towards the center

III. Long tail rogue wave clusters of Kuznetsov-Ma solitons

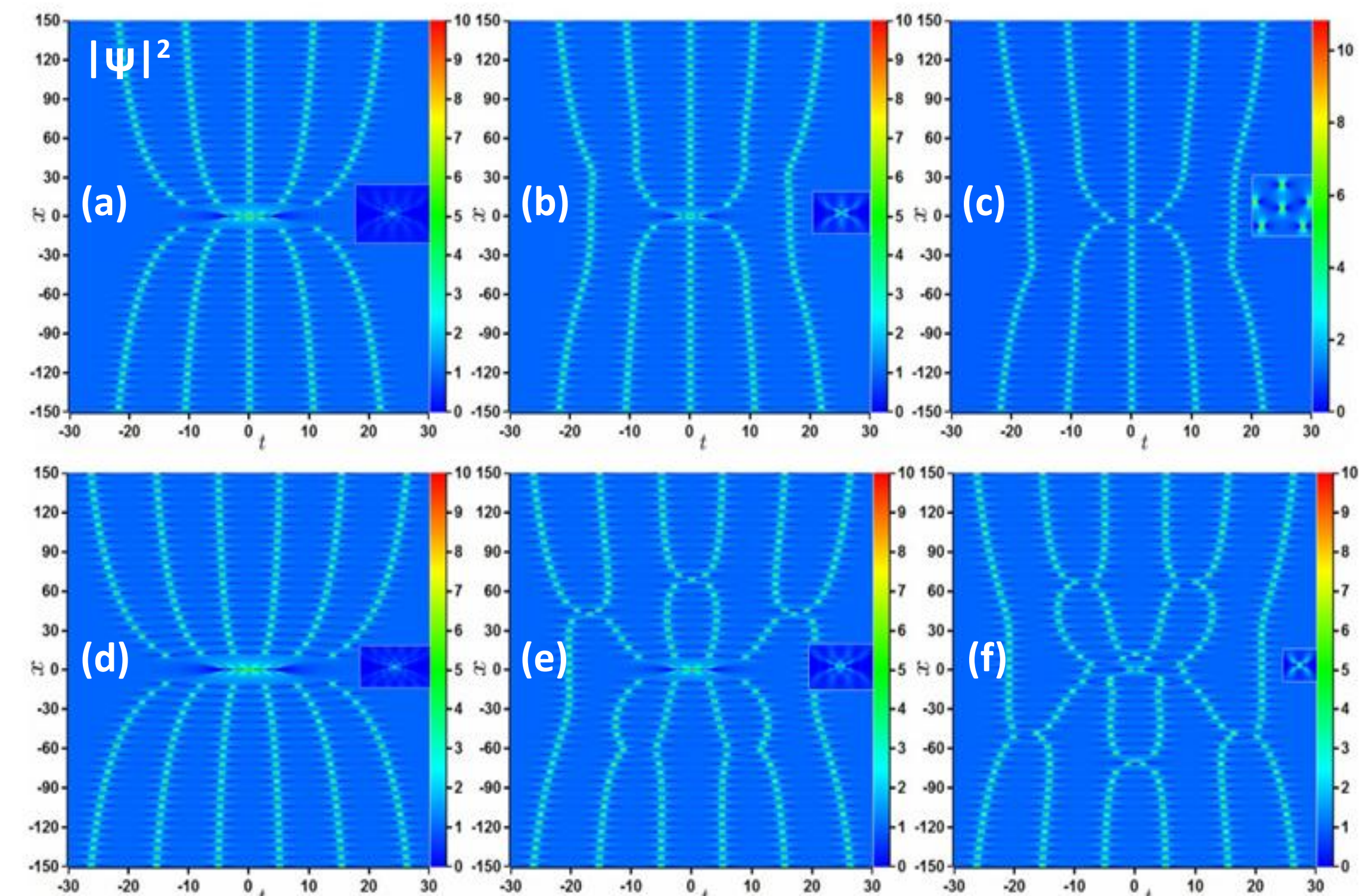


Figure 3: Long tail Kuznetsov-Ma clusters on uniform background for pure NLSE ($\alpha = 0, \gamma = 0, \delta = 0$) and $X_{j4}=10^6, \omega=0.05, v_0=0.1$: (a) $n=5, m=0$, (b) $n=5, m=1$, (c) $n=5, m=2$, (d) $n=6, m=0$, (e) $n=6, m=1$, (f) $n=6, m=2$.

Required:

1. noncommensurate frequencies,
2. evolution shifts

$$v_j = v_0 + \sqrt{1 - \frac{1}{4}j^2\omega^2}$$

- KMS of order $n-2m$ at (0,0) origin
- m tails with KMS1 above and below
- $m(m-1)$ KM1 loops above (below) just for even n

BTSC:

$$64\delta r^3 - 24\gamma r^2 - 8(\alpha + 2\delta + 8\delta v^2)r + 8\gamma v^2 + 4\gamma + 1 = 0$$

IV. Breather-to-soliton conversion (BTSC):

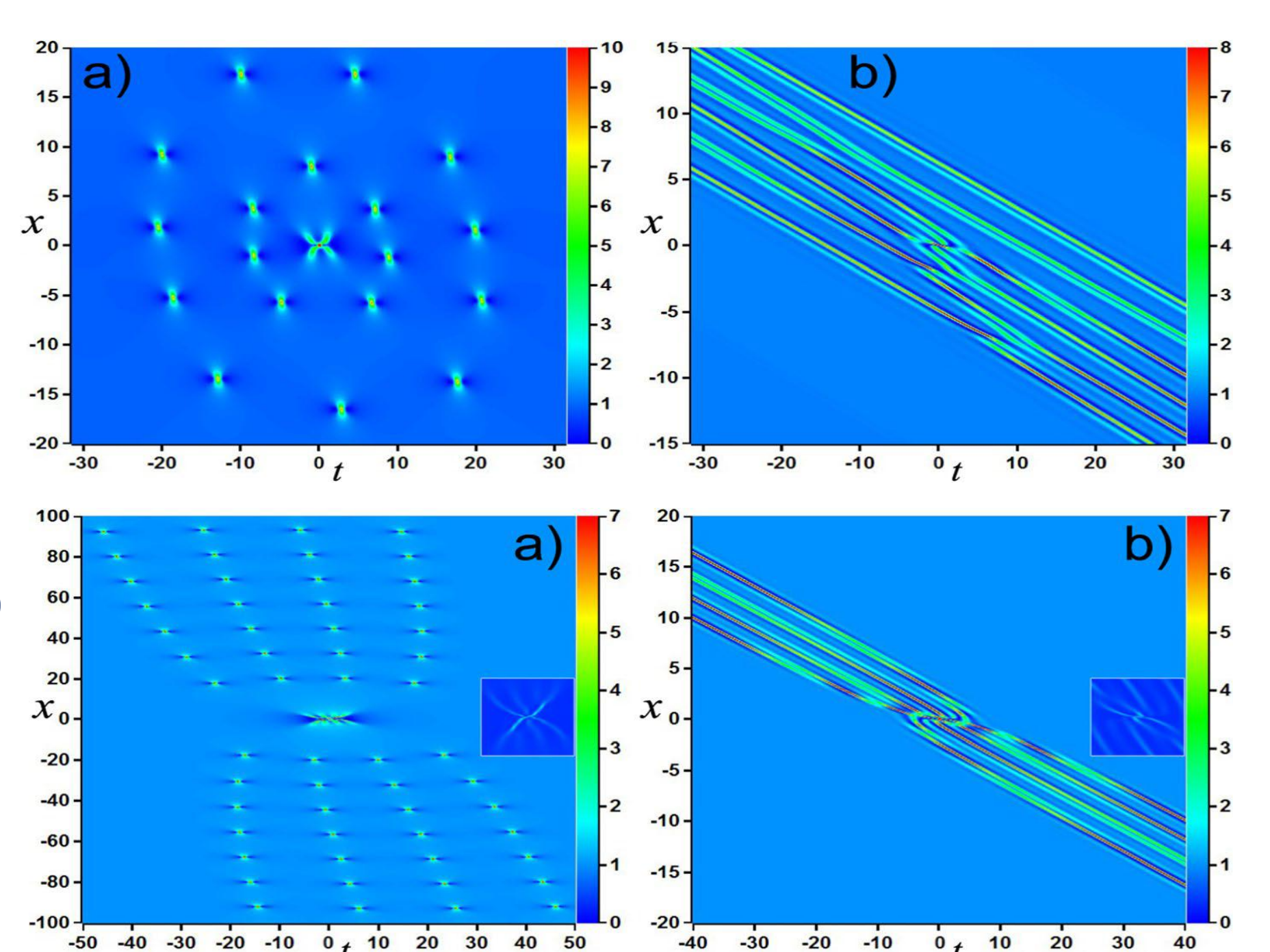


Figure 4 up: AB MERWC for $n = 6, m = 2, \omega = 0.1, x_1 = x_2 = 1, \alpha = 0.13, \gamma = 0.03, \delta = -0.02$. Real parts are: (a) = 0, (b) $\neq 0$.

Figure 4 down: KMS long tail clusters for $n = 4, m = 0, \omega = 0.05, v_0 = 0.02, \alpha = 0.13, \gamma = 0.03, \delta = -0.02$. Real parts are: (a) = 0, (b) $\neq 0$.